ORIGINAL PAPER

The effects of combined enzymatic and physical modifications of lentil protein applying Alcalase, Flavourzyme, microbial transglutaminase, and ultrasound: antioxidant, antihypertension, and antidiabetic activities

Amir Rezvankhah[1] · Mohammad Saeid Yarmand[1] · Babak Ghanbarzadeh[2]

Abstract

The enzymatically and physically modified lentil protein (LP) was assessed for antioxidant, antihypertension, and antidiabetic activities. First, Alcalase and Flavourzyme were sequentially used to produce lentil protein hydrolysate (LPH). Then, the LPH underwent microbial transglutaminase (MTGase)-mediated cross-linking (LPHC) and ultrasound treatment (LPHUS) individually and combinatory (LPHUSC). The amino acid composition, surface hydrophobicity (H_0), molecular weight (MW) profile and distribution, DPPH and ABTS radical scavenging activities (RSA), angiotensin-converting enzyme I-inhibitory (ACE), α-amylase, and α-glucosidase inhibitory activities, and functional properties were investigated. Results showed that the amino acid profiles were maintained after hydrolysis, cross-linking, and sonication while the residual values were slightly altered due to the centrifugation stages. Hydrolysis exposed the buried hydrophobic patches which led to a significant increase in H_0 while cross-linking reburied them which caused a remarkable reduction in H_0; Ultrasound also indicated a slight reducing effect in H_0. Sodium dodecyl sulfide polyacrylamide gel electrophoresis (SDS-PAGE) and gel permeation chromatography (GPC) results indicated that hydrolysis remarkably decreased the MW, cross-linking had an enlarging effect on peptides, and ultrasound disrupted the formed aggregates during hydrolysis. The hydrolysis increased DPPH and ABTS RSA while cross-linking had a decreasing effect on DPPH RSA and a slight increasing effect on ABTS RSA; Ultrasound indicated a slight reduction in DPPH RSA. The highest ACE, α-amylase, and α-glucosidase inhibitory activities were obtained for LPHC and LPHUSC. Also, LPHUSC indicated higher emulsifying activity and moderate stability. Consequently, LPHC and LPHUSC could be introduced as a potent mixture of peptides with antioxidant, antihypertension, and antidiabetic activities.

Keywords Lentil protein hydrolysate · Cross-linking · Sonication · ACE-inhibitory · α-Amylase · α-Glucosidase inhibitory

Introduction

The bad lifestyle, inappropriate food diets, and also genetic disorders have led to an increase in the patients who suffer from hypertension and diabetes type 2 [1–3]. The intention to use chemical drugs due to their side effects has decreased while using natural compounds with pharmacological impacts has been appealing [4–7]. Recently, the investigation of plant proteins has remarkably increased [8–10]. Especially, the modified plant proteins successfully have revealed potent biological and functional properties [1, 11, 12]. In this regard, plant protein hydrolysates have shown anti-hypertensive and antidiabetic effects as reported in the previous accomplished studies [9, 13]. These bioactive peptides due to their potent biological activities can be efficiently substituted by chemical drugs such as acarbose and voglibose [1, 2, 14]. Besides, they can be substituted by antihypertensive drugs and chemical antioxidants in food formulations [14–16]. The bioactivity of peptides is directly related to their molecular size, amino acid composition, and

✉ Mohammad Saeid Yarmand
yarmand.m.s@gmail.com

1 Department of Food Science and Technology, Razi Food Chemistry Lab, College of Agriculture and Natural Resources, University of Tehran, Karaj, Iran

2 Department of Food Science and Technology, Faculty of Agriculture, University of Tabriz, Tabriz, Iran

amino acid sequences [10, 14, 17]. So, the production of bioactive peptides from plant protein sources has become the case study of several researchers [9, 10].

Hydrolysis of plant proteins is accounted as one of the ways to modify their structures [9, 10, 18]. However, the extent of hydrolysis is a substantial issue, and a higher or lower degree of hydrolysis (DH) can alter the peptide bioactivity [9, 10, 19]. Acidic hydrolysis has been introduced as an abolished method due to the production of carcinogenic compounds such as 3-Chloropropane-1,2-diol (3-MCPD) [9, 20]. Acidic hydrolysis is an intensive reaction (using HCl at 6 M) that produces peptides with uncontrolled DH which rises to higher than 50% [21, 22]. Due to applying high temperature (above 110 °C) and intensive acidic condition (pH ~2.0), carcinogenic compounds are produced and amino acids are undergone chemical reactions leading to reduction of peptides bioactivity [9, 10]. Enzymatic hydrolysis of proteins is performed by proteolytic enzymes such as Alcalase, Flavourzyme, pepsin, pancreatin, bromelain, ficin, etc. [15, 23, 24]. These enzymes find the specific site of proteins, break down the peptide bonds, and liberate peptides with different bioactivity; Hence, limited and controlled DH value can be obtained [25, 26]. Alcalase and Flavourzyme are hydrolyzing enzymes that are extensively used in umami-taste production companies [9, 27]. Alcalase widely hydrolyzes the protein structure and is an endopeptidase that cleaves the protein through the inner section [28]. The produced peptides via Alcalase have mostly shown higher DH (> 10%) and also higher antioxidant and biological activities [29, 30]. Rezvankhah et al. [9, 10] reported that lentil protein hydrolysate obtained by Alcalase indicted higher angiotensin I-converting enzyme (ACE) inhibitory activity than non-hydrolyzed protein. Similar results were reported by Garcia-Mora et al. [31, 32] and Barbana et al. [33, 34] for lentil protein hydrolysates. Also, the associated enzymes in diabetes mellitus, α-glucosidase, and α-amylase have been efficiently inhibited by the hydrolysates produced by Alcalase [1, 35, 36]. It was reported that potato protein hydrolysates obtained by Alcalase exhibited α-glucosidase and α-amylase inhibitory activities [36]. Similar results were found for Changii Radix protein hydrolysates under the optimal enzymatic hydrolysis conditions of trypsin, Flavourzyme, compound proteinase, papain, alkaline proteinase, and neutral protease [25]. When the Alcalase is used sequentially with Flavourzyme as endo- and exopeptidase enzyme (or other secondary enzymes), the produced hydrolysates have shown higher biological activity likely due to their small molecular weight (MW) [10, 37, 38]. Most of the plant protein hydrolysates have shown higher antioxidant activity compared to native proteins [1, 9, 18].

Lentil (*Lens culinaris*) is one of the pulse proteins which has shown good functional properties [39, 40]. It has 21–31% wt protein with a dominant portion of storage proteins (80% wt) [31, 40, 41]. Its protein is comprised of legumins with MW of 350–400 kDa and vicilins with MW of 150–200 kDa as the two main globulins [9, 10, 37]. Also, prolamins and glutelins are a minority present in lentil protein [9, 39]. Enzymatic hydrolysis of lentil protein (LP) has produced bioactive peptides with antioxidant and ACE-inhibitory activities [9, 31]. Various studies have shown that lentil protein hydrolysate (LPH) can be potentially used as an anti-hypertensive compound [9, 10, 31, 39]. However, there were no reports regarding the antidiabetic properties of LPH.

Enzyme modification is not only the hydrolysis of proteins but also cross-linking by a microbial transglutaminase (MTGase) through catalyzing the acyl-transfer reactions between γ-carboxyamine groups of peptide-bound glutamyl residues and a range of primary amino groups, has been also considered the protein's structure enzymatic modification [42, 43]. When the amine-containing substrate is the ε-amino group of a peptide-bound lysyl residue, peptide chains can be covalently connected through ε-(γ-glutamyl) lysine isopeptide bonds [23, 44]. MTGase reaction has been reported to increase the MW and improve solubility and interfacial properties of hydrolysates [23, 44]. After MTGase catalyzing, it has been reported that the content of peptides with MW of 1000–5000 Da was increased and higher umami taste with a reduction of bitterness (by masking) was developed [45]. The bitterness of produced cross-linked peptides was decreased by post-hydrolysis cross-linking when MTGase was used in a combination with Alcalase [44, 46]. Also, scavenging capabilities were detected for glycopeptides obtained by proteolysis from corn gluten meal followed by transglutaminase-induced glycosylation with glucosamine [47]. No further studies were observed regarding the antihypertensive and antidiabetic effects of MTGase.

Physical modifications such as heating, freeze-thawing have also shown significant effects on the protein structures [48]. The novel non-thermal processing methods have been extensively used recently due to their high efficiency in modifications [11, 49]. Ultrasound is one of the non-thermal strategies in the physical modification of protein structures [50]. The acoustic cavitation of ultrasound can rupture/disintegrate the aggregated polypeptides, alter the protein's secondary structure, and change the biological activities of proteins and peptides [29, 51–53]. Unraveling of protein's structure can also lead to improved functional characteristics [4, 29, 54]. Besides, increased antioxidant activity, ACE, α-amylase, and α-glucosidase inhibitory activities have been reported for proteins exposed to ultrasound pretreatment and then enzymatically hydrolyzed [15, 29, 53, 55].

This study was performed to evaluate the post-MTGase-mediated cross-linking and ultrasound treatment on the sequentially hydrolyzed lentil protein by Alcalase and Flavourzyme. The effects were investigated on antioxidant

activity, ACE, α-amylase, and α-glucosidase inhibitory activities, and functional properties via the evaluation of amino acid composition, surface hydrophobicity, and MW changes.

Material and methods

Materials

Lentils were provided from the local market of Karaj (Iran). Alcalase 2.4 L with a specific activity of 2.4 Anson Units (AU)/g and Flavourzyme 1000 L with a specific activity of 1000 leucine aminopeptidase unit (LAPU)/g were purchased from Novozymes Co. (Bagsvaerd, Denmark). MTGase with the activity of 100 U/g was supplied by Ajinomoto Co. (Foods Europe S.A.S, EMB 80585A, France). Angiotensin I-converting enzyme (ACE) from rabbit lung and the ACE synthetic substrate hippuryl-L-histidyl-L-leucine (HHL) were purchased from Sigma–Aldrich Canada Ltd. (Oakville, ON, Canada). Porcine pancreatic α-amylase (Cat no. A3176) and rat intestinal α-glucosidase (Cat no. I1630) were purchased from Sigma-Aldrich Co. (St. Louis, Mo, USA). Other chemicals used were analytical grade and provided by Sigma-Aldrich Co. (St. Louis, Mo, USA) or Merck Co. (Darmstadt, Germany).

Preparation of hydrolysate

Lentil protein hydrolysate (LPH) was generated according to the method described by Rezvankhah et al. [10]. Briefly, lentil protein (LP) solution at 3% wt was prepared from the produced spray-dried powder obtained by the alkalization-precipitation procedure [9, 56]. Then, the LP solution was heated at 95 °C for 15 min to unfold the protein's structure and cooled down to the optimal temperature of Alcalase activity (60 °C). The enzymatic hydrolysis was initiated using Alcalase (at pH 8.0) at the enzyme to the substrate (E:S) of 2% wt for 120 min; Then, the enzyme was terminated by heating the solution at 90 °C for 15 min [9, 10]. The hydrolysate solution was cooled down to 50 °C as the optimal temperature of Flavourzyme activity. The secondary hydrolysis stage was started by the Flavourzyme addition at pH 7.0 and E:S of 2% wt for 60 min and then the enzymatic reaction was stopped by heating at the mentioned condition. The optimal pH conditions were maintained by dropping 2 N NaOH solution. The hydrolysate solution was centrifuged at 15,000×*g* for 15 min and the obtained supernatant rich in soluble peptides was collected and spray-dried using a mini spray-dryer (FAnyuan Instrument, FYI, SP-1500, China) at inlet temperature of 160 °C, outlet temperature of 80 °C, and air compressor pressure of 0.3 MPa [56]. The spray-dried

hydrolysate was termed lentil protein hydrolysate (LPH) and stored at 4 °C.

Degree of hydrolysis (DH)

DH (%) of LPH was measured based on the pH–stat method described by Rezvankhah et al. [9]. Accordingly, the pH of enzymatic hydrolysis was maintained constant by continuous addition of 2 N NaOH solution (mL) and its consumption was recorded. The DH was measured using the equation below [9, 10]:

$$DH(\%) = B \times N_b \times \frac{1}{\alpha} \times \frac{1}{M_P} \times \frac{1}{h_{tot}} \tag{1}$$

where B was the volume of consumed NaOH solution; N_b was the normality of basic solution; M_p was the mass of protein in LP powder; h_{tot} was the total number of peptide bonds in the protein substrate (considered 7.78); α was the NH$_2$ groups released during the hydrolysis and computed using the equation below:

$$\alpha = \frac{10^{pH-pk}}{1 + 10^{pH-pk}} \tag{2}$$

where pK was the average pK-value of α-NH$_2$ groups liberated. pH was the optimum pH activity of enzymes used in hydrolysis. The pK was the temperature-dependent parameter and was calculated by the following relation:

$$pk = 7.8 + \left(\frac{298 - T}{298T} \right) \times 2400 \tag{3}$$

where T (Kelvin, K) was the temperature of enzymatic hydrolysis.

Cross-linking of LPH

The MTGase-mediated cross-linking was conducted according to the established method of Song et al. [45] with slight modifications. First, LPH solution at 10% wt was prepared and allowed to be hydrated for 30 min. Then, the pH of the solution was adjusted to 8.0, and the temperature was set at 45 °C. MTGase was added at E:S of 1.2% wt and the reaction was performed for 5 h. After then, the enzyme was terminated at 95 °C for 10 min and the solution was centrifuged at 11,300×g for 10 min at 25 °C. The supernatant was collected and spray-dried at the mentioned conditions of the last section and termed lentil protein hydrolysate cross-linked (LPHC). The produced sample was stored at 4 °C.

Ultrasound treatment of LPH

The ultrasound treatment of LPH was carried out using the method of Tian et al. [53] with slight modifications. LPH

solution (10%) was subjected to an ultrasound probe system (TopSonics UPH-400), with 400 W output power at 20-kHz frequency, an amplitude of range ~of 83–95 μm, and a flat-tip probe diameter (Horn) of 12 mm. The sonication was conducted at 150 W for 10 min at the interval conditions of 2 s on and 2 s off. The temperature of the LPH solution was controlled using an ice bath. The sonicated LPH solution was centrifuged at 10,000×g for 20 min and the supernatant was collected and spray-dried at the abovementioned conditions. The ultrasound-treated LPH was termed LPHUS. Also, LPHUS underwent the MTGase-mediated cross-linking process and the obtained cross-linked sample was termed LPHUSC. The produced samples were stored at 4 °C.

Characterization of produced hydrolysates

Amino acid composition

The amino acid profile of LP, LPH, LPHC, LPHUS, and LPHUSC was determined using the method suggested by Rezvankhah et al. [9]. Accordingly, reverse-phase high-performance chromatography (RP, Agilent 1100 HPLC; Agilent Ltd., Palo Alto, CA, USA) was applied to determine the total amino acid composition. First, the samples underwent HCl hydrolysis (6 N) at 120 °C for 22 h in the glass tubes filled with nitrogen. The hydrolyzed samples then were transferred into 25 mL volumetric flasks and neutralized with NaOH 10 N. The obtained hydrolysate samples were filtered through the two layers of filter paper No. 40, and the filtrates were transferred to the centrifuge tubes and centrifuged at 1000×g for 10 min. A volume of 400 μL of each sample was taken and transferred into an injection bottle. The injection program was as follows: each sample was injected into a Zorbax, 80 A C-18 column (with the size of 4×250 mm, 5 μm particle size; Agilent, USA) at 40 °C with detection at 338 nm. For elution of the column, two series of mobile phases were used. The mobile phase A was comprised of 7.35 mM/L of sodium acetate/triethylamine/tetrahydrofuran (500:0.12:2.5, v/v/v), adjusted to pH 7.2 using acetic acid. The mobile phase B was comprised of 7.35 mM/L of sodium acetate/methanol/acetonitrile (1:2:2, v/v/v), adjusted to pH 7.2. For quantification of amino acids, a standard solution containing 17 amino acids was also injected into the column as an external standard.

Surface hydrophobicity

The H_0 of LP, LPH, LPC, LPHUS, and LPHUSC was determined according to the method of Ashraf et al. [57] with slight modifications. Accordingly, 1-anilino-8-naphthalene sulfonate (ANS) was used as the hydrophobic fluorescence probe. Briefly, 4 mL of sample solution (0.2–1 mg/mL) was mixed with 20 μL (8 mM) of freshly prepared ANS solution. The mixture was vigorously shaken by a vortex and stored at room temperature in darkness. The fluorescence (FI) of each sample was recorded at 280 nm as excitation and 350 nm as emission using a fluorometer (F-2500; Hitachi, Tokyo, Japan). The H_0 value was computed by the linear regression from the initial slope of the plot of net FI versus protein/peptide concentration (mg/mL).

MW profile

The polypeptide profiles of LP, LPH, LPHC, LPHUS, and LPHUSC were determined using sodium dodecyl sulfide polyacrylamide gel electrophoresis (SDS-PAGE) according to the method described by Avramenko et al. [58]. Briefly, the sample concentration of 0.5% (v/v) (75 μL of 1% sample in 75 μL water) was used for SDS-PAGE analysis. Then, 150 μL of each sample were transferred into separate Eppendorf tubes followed by the addition of 150 μL of Laemmli sample buffer. Before the electrophoresis, the samples were heated at 95 °C for 10 min and centrifuged at 12,000×g for 5 min. The molecular weight standards (Bio-Rad Broad Range Marker) were also run in conjunction with samples on Bio-Rad Tris–HCl gel (15%) at 100–110 V for 1.5 h. The protein bands were stained using Coomassie blue R-350.

MW distribution

MW distribution of LP, LPH, LPC, LPHUS, and LPHUSC was determined using the method of Rezvankhah et al. [10]. Gel permeation chromatography system (GPC, Waters Breeze HPLC system, Waters Corporation, Milford, MA, USA) equipped to Waters UV detector and Superdex Gel filtration column, phase Superdex Peptide HR (length × internal diameter 30 cm × 10 mm and 13–15 μm particle size) was applied to determine MW distribution. The samples were dissolved in ultrapure water and then centrifuged at 12,000×g for 10 min. The supernatants were collected and filtered through a 0.22 μm membrane. The filtered solution was transferred into an analysis bottle and 50 μL of each sample was injected into the column. The isocratic elution process was considered for the column and 0.02 M phosphate buffer containing 0.25 M NaCl (pH 7.2) was used as the mobile phase at a flow rate of 0.5 mL/min. To determine the MW distribution of samples, the MW calibration curve was plotted using standards with specific retention times. The applied standards were Cytochrome C, Aprotinin, Cyanocobalamin, Glutathione disulfide, and Glutathione reduced. The MW distribution of samples was obtained according to the comparison of the volume of the eluted peaks with the standard elution volumes.

Antioxidant activity

DPPH radical scavenging activity

DPPH radical scavenging activity assay was carried out according to the method of Rezvankhah et al. [9]. First, a reaction mixture containing 2 mL of each sample solution (7 mg/mL) and 2 mL of DPPH ethanolic solution (0.2 mM) was prepared. The mixture was kept in darkness for 30 min and then the absorbance value was recorded using a UV–vis spectrophotometer (SP-UV 500DB spectrophotometer, Spectrum instruments, Canada). Ascorbic acid (0.01 mg/mL) was also used as the positive control. The radical scavenging activity percentage (RSA%) was determined by the following equation [9]:

$$RSA(\%) = \frac{A_C - A_S}{A_C - A_B} \times 100 \tag{4}$$

where A_C, A_S, and A_B indicated the absorbance values of control, sample, and blank.

ABTS radical scavenging activity

The 2,2′-azinobis (3-ethylbenzothiazoline-6-sulfonate) radical cation (ABTS$^{·+}$) scavenging activity of LP, LPH, LPHC, LPHUS, and LPHUSC was determined according to the method of Ambigaipalan et al. [59] with slight modifications. ABTS$^{·+}$ was prepared by oxidizing a 5 mmol/L aqueous solution of ABTS with manganese dioxide at ambient temperature for 30 min. The absorbance of ABTS$^{·+}$ solution was adjusted to 0.7 at 734 nm. Then, 50 μL of each sample solution (7 mg/mL) were mixed with 950 μL of ABTS$^{·+}$ solution and after a 10 min reaction, the absorbances were determined using a UV–vis spectrophotometer. The ABTS$^{·+}$ radical scavenging activity was measured by the equation mentioned in the previous section.

ACE-inhibitory activity

The angiotensin I-converting enzyme (ACE) inhibitory activity of LP, LPH, LPHC, LPHUS, and LPHUSC was determined according to the method established by Ambigaipalan et al. [59] with slight modifications. The samples and enzyme were dissolved in 50 mM HEPES-HCl buffer containing 300 mM NaCl (pH 8.3). The 10 μL of samples (0.1–2 mg/mL) were mixed with 20 μL of ACE solution (0.25 unit/mL). The mixture was pre-incubated at 37 °C for 5 min. The reaction was initiated by dissolving 50 μL of HHL (6 mg/mL) in distilled water and added to the mixture followed by incubating at 37 °C for 15 min. The hippuric acid formed was extracted with 1 mL of ethyl acetate. The mixture was centrifuged at 1200×g for 5 min. The obtained supernatant was collected and placed in boiling water to remove ethyl acetate. The hippuric acid retained was dissolved in 1 mL of distilled water and the absorbance was measured at 228 nm. The control was prepared using 50 mM HEPES-HCl buffer containing 300 mM NaCl (pH 8.3) instead of the sample. Also, the sample blank and control blank were run in the same manner, except that ACE solution was added to the reaction before the addition of 1 M HCl. The ACE-inhibitory activity (%) was calculated using the equation below [59]:

$$Inhibitory\ activity(\%) = \frac{A_C - A_S}{A_C - A_B} \times 100 \tag{5}$$

where A_C was the absorbance of the control, A_S was the absorbance of the sample, and A_B was the absorbance of the blank. The IC_{50} values were also calculated based on the prepared serial concentrations. The IC_{50} of ACE-inhibition meant that the least concentration of samples was needed to inhibit the enzyme.

α-amylase inhibitory activity

The α-amylase inhibition assay was carried out based on the suggested method of Karimi et al. [3] with slight modifications. Briefly, 100 μL of sample solution (10–500 μg/mL) were mixed with 100 μL of α-amylase solution (0.5 U/mL) and incubated at 37 °C for 5 min. After preincubation, 100 μL of 0.5% (w/v) starch solution were added and the obtained reaction mixture was incubated at 37 °C for 20 min. Then, the reaction mixture was heated at 100 °C for 10 min and then cooled down to the ambient temperature followed by centrifuging at 15,000×g for 2 min to separate the undigested starch. Then, 20 μL of supernatant were mixed with 1 mL of PAHBAH and heated to 70 °C for 10 min. The solution was cooled down to room temperature and absorbance was read at 410 nm. Acarbose was also used as the positive control. The α-amylase inhibitory activity was measured using the equation below [3]:

$$Inhibition\ of\ \alpha - amylase\,(\%) = \left(1 - \frac{(A_S - A_B)}{A_C} \right) \times 100 \tag{6}$$

where A_S, A_B, and A_C represented the absorbance of sample, blank (phosphate buffer, enzyme, sample), and control (starch, buffer, enzyme), respectively. Also, IC_{50} values were measured by preparation of serial concentrations. It was meant that the least concentration of samples could inhibit 50% activity of the enzyme.

α-glucosidase inhibitory activity

The α-glucosidase (rat intestinal) inhibitory activity of LP, LPH, LPHC, LPHUS, and LPHUSC was measured according to the method of Karimi et al. [3] with slight modifications. The enzyme was extracted from rat intestinal acetone powders and then diluted to 90 mU/mL. Then, 100 μL of sample solution (10–500 μg/mL) were mixed with 200 μL of α-glucosidase and incubated at 37 °C for 10 min. After preincubation, 5 mM PNPG solution (100 μL) were added and incubated at 37 °C for 10 min. The absorbance of the solution was read every 2 min at 405 nm. The phosphate buffer was also used as a control instead of a sample solution. Acarbose was also used as the positive control. The enzyme inhibitory activity was measured using the relation below [3]:

$$Inhibtion\ of\ \alpha - glucosidase\ (\%) = \frac{A_C - A_S}{A_C} \times 100 \qquad (7)$$

where A_C and A_S represented the absorbance of control and sample, respectively. IC_{50} values were also determined for protein and peptides by preparation of serial concentrations. It was meant that the least concentration of protein and bioactive peptides could inhibit 50% of enzyme activity.

Functional properties

Solubility

The solubility of LP, LPH, LPHC, LPHUS, and LPHUSC was determined according to the method described by Rezvankhah et al. [10]. The samples were prepared at 10 mg/mL at pH values of 4.0, 7.0, and 9.0 and centrifuged at 8000×g for 15 min. The protein content of the supernatant was determined using the Bradford method. Bovine serum albumin (BSA) was used to plot the standard curve. The solubility was calculated using the following equation [10]:

$$Solubility(\%) = \frac{Protein\ content\ in\ the\ supernatant}{Total\ protein\ content\ in\ the\ sample} \times 100 \qquad (8)$$

Emulsifying properties

The emulsifying activity index (EAI, m²/g) and emulsifying stability index (ESI, min) were determined using the method suggested by Rezvankhah et al. [10]. The samples at the concentration of 10 mg/mL were prepared and then mixed with 1 mL of sunflower oil followed by homogenization at 19,000 rpm for 1 min using a laboratory-scale homogenizer (IKA, T25, Staufen, Germany). To determine EAI, 50 μL of

the emulsion were taken from the bottom of the container immediately after emulsion fabrication. To determine ESI, 50 μL of the emulsion were taken from the bottom of the container after 10 min storage of emulsion. The taken volumes were mixed with 5 mL of SDS (0.1%) and diluted solutions were evaluated for their absorbances at 500 nm using a spectrophotometer. EAI and ESI were computed from the equations below [10]:

$$EAI\left(\frac{m^2}{g}\right) = \frac{(2)(2.303)(A_0)(DF)}{(I)(\theta)(C)} \qquad (9)$$

$$ESI(\text{min}) = \frac{A_0}{\Delta A}\Delta t \qquad (10)$$

where A_0 indicates the absorbance of diluted emulsion at 500 nm immediately after homogenization, DF = dilution factor (100), I = path length of the cuvette (m), θ indicates the oil volume fraction (0.25), C = protein concentration in the aqueous phase (g/m³), $\Delta A = A_0 - A_{10}$, $\Delta t = 10$ min.

Foaming properties

The foaming capacity (FC) and foaming stability (FS) of the LP, LPH, LPHC, LPHUS, and LPHUSC were determined according to the method of Rezvankhah et al. [10]. The samples at 10 mg/mL were prepared and then whipped at 19,000 rpm for 2 min with a laboratory-scale homogenizer (IKA, T25, Staufen, Germany). The whipped solutions were transferred into a 50 mL graded cylinder and the total volumes were determined. Also, they were allowed to stand for 30 min at 20 °C, and then the total volumes were recorded. FC and FS were calculated using the following equations [10]:

$$FC(\%) = \frac{B - A}{A} \times 100 \qquad (11)$$

$$FS(\%) = \frac{C - A}{A} \times 100 \qquad (12)$$

where A, B, and C indicate the volume of protein or peptide solutions before being whipped (mL), the volume immediately after whipping (mL), the volume after standing for 30 min (mL), respectively.

Statistical analysis

All experiments were accomplished at three replications and data were reported with means and standard deviations. The statistical analysis of the results was conducted by one-way ANOVA. The mean difference of data was assessed by the Duncan test using the SPSS software (version 23, IBM software, NY, USA).

Results and discussion

The hydrolysis of LP was conducted sequentially to produce bioactive peptides with high biological activities [10, 60]. First, LP was hydrolyzed by Alcalase and DH reached 17.5% after 120 min. Alcalase can produce polypeptides with medium and small-sized polypeptides through the inner part of the protein [9, 26, 28]. Then, Flavourzyme continued the hydrolysis process for a further 60 min and cleaved the produced peptides by Alcalase and DH reached 36%. Similar results were found in the previous studies [9, 10]. Indeed, when Alcalase hydrolyzed the protein, the initial structure of the protein was unraveled and peptides with the associated specific sites were highly matched with the active site of Flavourzyme, and extensive hydrolysis occurred [10, 61]. Sequential hydrolysis has been reported to significantly increase the DH, increase the biological activities, and reduce the bitterness of produced peptides [9, 27, 38, 62]. In other words, the combined hydrolyzing enzymes can more efficiently increase the DH and subsequently produce peptides with stronger biological activities [28, 59, 63]. The produced LPH underwent the MTGase-mediated cross-linking process and also was treated with ultrasound individually and combined with cross-linking [53, 64]. It was hypothesized that hydrolysis, cross-linking, and ultrasound treatment could show a significant effect on the antioxidant activity, ACE, α-amylase, and α-glucosidase inhibitory activities, umami taste development, and functional properties. The effects could be associated with the changes in MW profile and distribution, conformation, surface hydrophobicity, and hydrophilicity [4, 13, 23, 38, 64].

Amino acid composition

The amino acid composition of samples was determined using RP-HPLC and the obtained results were provided in

Table 1 RP-HPLC amino acid profiles of LP, LPH, LPHC, LPHUS, and LPHUSC

Amino acid composition (%w/w)	LP	LPH	LPHC	LPHUS	LPHUSC
Aspartic acid (Asp)	12.02	13.01	11.92	11.61	11.33
Serine (Ser)	5.35	4.59	5.49	5.23	4.98
Glutamic acid (Glu)	15.76	17.07	17.52	15.45	15.03
Glycine (Gly)	4.43	4.26	3.94	4.42	4.13
Histidine (His)	2.02	1.81	2.17	2.35	2.19
Arginine (Arg)	6.59	7.67	7.43	6.65	6.72
Threonine (Thr)	3.88	4.41	3.76	3.19	2.82
Proline (Pro)	4.73	5.40	5.81	6.28	5.54
Alanine (Ala)	4.21	4.52	4.74	5.10	4.89
Cystine (Cys)	1.51	1.30	1.44	1.31	1.61
Tyrosine (Tyr)	3.26	2.64	2.91	3.25	3.69
Valine (Val)	4.88	4.38	4.58	4.81	4.27
Methionine (Met)	1.73	1.47	1.91	1.80	1.73
Lysine (Lys)	8.56	7.73	8.32	8.65	8.19
Isoleucine (Ile)	3.86	3.45	3.60	3.11	2.87
Leucine (Leu)	8.98	9.35	9.17	9.76	9.70
Phenylalanine (Phe)	4.53	4.13	3.60	3.20	2.53
Amino acid residue yield (%)	96.29	97.19	98.29	96.17	92.21
Total essential amino acids	38.44	36.73	37.11	36.87	34.3
Total non-essential amino acids	57.86	60.46	61.2	59.3	57.92
Hydrophobic amino acids	38.86	38.26	38.79	39.79	37.27
Hydrophilic amino acids	14	12.94	13.6	12.98	13.1
Positively charged amino acids	17.17	17.21	17.92	17.65	17.1
Negatively charged amino acids	27.78	30.08	29.44	27.06	26.36
Sulfur-containing amino acids	3.24	2.77	3.35	3.11	3.34
Umami amino acids	38.74	41.81	42.16	40.79	38.98

Essential amino acids include His, Ile, Leu, Lys, Met, Phe, Thr, and Val. Non-essential amino acids include Asp, Ser, Glu, Gly, Arg, Pro, Ala, Cys, and Tyr. Hydrophobic amino acids include Ala, Val, Ile, Leu, Phe, Pro, Met, Cys, and Gly. Hydrophilic amino acids include Ser, Thr, Cys, and Tyr. Positively charged amino acids include Arg, His, and Lys. Negatively charged amino acids include Asp and Glu. Sulfur-containing amino acids include Met and Cys. Umami amino acids include Asp, Glu, His, Pro, and Ala

Table 1. The initial look at the amino acid table exhibited that hydrolysis, cross-linking and ultrasound did not have a significant effect on the main amino acid composition of LP. Asp, Ser, Glu, Gly, Arg, Pro, Ala, Val, Lys, Leu, and Phe were detected mostly higher than 4% wt in the LP and processed hydrolysates [9, 10]. Most of these amino acids are the main contributors to biological activities [10, 29]. Alcalase had a broad specificity for methionine, leucine, serine, and alanine. The produced hydrolysates by Alcalase have shown a high amount of these amino acids depending on the protein source while Flavourzyme hydrolysates have been reported to be richer in glutamic acid, arginine, and isoleucine [15]. Hence, the sequential hydrolysis led to the production of a high amount of those amino acids.

According to Table 1, a slight difference within the amino acid residue yields was possibly related to the separation of polypeptides during the centrifugation, either in the production of LP that some polypeptides were separated in the alkalization stage or the production of LPH that unhydrolyzed polypeptides were separated. Besides, the production of LPHC, LPHUS, and LPHUSC had centrifugation processes, thereby unprocessed proteins were separated [15, 65–67]. The same explanation was presented by You et al. [67] and Fadimu et al. [15] that some dipeptides and larger peptides may fail to be hydrolyzed. Separation of unprocessed proteins led to slight differences in the essential amino acid contents (Table 1). The highest content of essential amino acids was obtained for LP while the lowest content was obtained for LPHUSC (Table 1). This phenomenon could be related to the several centrifugation stages that LPHUSC underwent. Despite this, LP and also its processed products indicated acceptable essential amino acid contents which should be delivered according to the daily intake suggested by FAO/WHO [15, 65]. This implied that the produced hydrolysates (LPH, LPHC, LPHUS, and LPHUSC) had good potential to be used as a dietary protein supplement in foods.

The dominant part of LP and produced hydrolysates was assigned to the hydrophobic amino acids including Ala, Val, Ile, Leu, Phe, Pro, Met, Cys, and Gly (Table 1) [9, 10]. The higher hydrophobic amino acid content was achieved for LPHUS related to the centrifugation processes and supernatant polypeptides [15]. Ultrasound solubilized the peptides and exposed the hydrophobic segments, thereby higher hydrophobic amino acids were detected [64]. Albeit, the hydrophobic amino acids cannot individually show the hydrophobicity of peptides [10]. The sequence of amino acids in the peptides and more specifically the amino acid at the end residue of the peptide can also affect the hydrophobicity, hydrophilicity, and other biological activities [68]. Total amino acid composition by RP-HPLC indicated just amino acids constructed the protein or peptides' initial structures [9]. Further, hydrolysis, cross-linking, and sonication

can change the MW of peptides; thus, different amino acid compositions can be provided [69]. Also, some amino acids inherently have been accepted as an antioxidant [9, 10]. Asp, Glu, Lys, Pro, Leu, Val, Phe, His, Tyr, Lys, and Met are such amino acids. However, their position in the peptide chain can substantially affect the peptide's biological activities [15].

Higher positively charged amino acids were obtained for LPHC and LPHUS while higher negatively charged amino acids were achieved for LPH and LPHC (Table 1). These amino acids including Arg, His, Lys, Asp, and Glu have been known as an antioxidant and also umami-taste contributor amino acids [10, 70]. Sulfur-containing amino acids altered after hydrolysis and the highest amounts were detected for LPHC and LPHUSC, which can render higher meat analog flavor [45, 71].

Surface hydrophobicity

The H_0 values of LP, LPH, LPHC, LPHUS, and LPHUSC were represented in Fig. 1. The surface hydrophobicity has important influences on the macromolecular structural stability, surface property, and fat-binding ability of protein [58, 72]. Also, possessing surface hydrophobicity has been introduced as a prerequisite for appreciable surface activity [73]. ANS has been known as one of the most popular types of fluorescence probes which may combine or interact with the aromatic amino acid residues [73]. Non-hydrolyzed LP indicated a moderate surface hydrophobicity likely due to the presence of hydrophobic peptides in its protein mixture [58]. LP has been reported to show higher interfacial properties due to containing hydrophobic proteins [74, 75]. LP has also shown high comparable interfacial attributes with
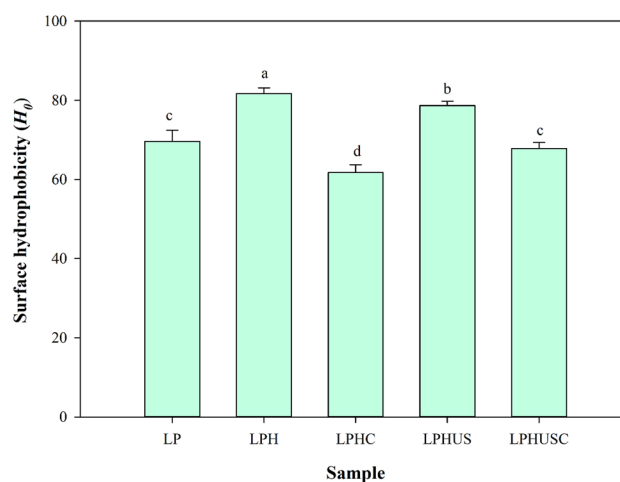

Fig. 1 Surface hydrophobicity (H_0) values of LP (control), LPH, LPHC, LPHUS, and LPHUSC. LP was native lentil protein; LPH was Alcalase-Flavourzyme hydrolysates; LPHC was MTGase cross-linked LPH; LPHUS was treated LPH with ultrasound; LPHUSC was LPH treated with ultrasound and MTGase

animal-based proteins such as sodium caseinate, whey protein concentrate, and BSA [75]. Based on the reports, LP has shown higher surface hydrophobicity than sodium caseinate, whey protein concentrate, and lysozyme [75]. According to Fig. 1, it was observed that hydrolysis led to a significant increase in surface hydrophobicity for LPH [15, 76]. This increase could be associated with the unraveling of protein structure and exposing the buried hydrophobic patches [15]. Indeed, Alcalase-Flavourzyme combined hydrolysis system led to the liberation of peptides with small- and medium-sized properties and also exposed hydrophobic surfaces [15, 76]. Hydrolysis has shown declining effects on disulfide (SS) bonds which were found to be significantly lower than that of intact protein. Disulfide bonds might be the driving force required to approach and maintain together with the protein chains [73]. On another side, it has been declared that the high content of SS bonds, the non-covalent interactions, particularly the hydrophobic interactions are important for the aggregation tendency of a protein although they are not the driving force for the aggregation process [73]. When LP was hydrolyzed, the H_0 reached the highest value (Fig. 1) within the present samples due to the unfolding of the main structure, and the production of lower MW peptides with exposed hydrophobic segments that highly interacted with the ANS probe [58, 73]. The current findings were in agreement with those reported for hydrolysis of corn glutelin by Protamex and walnut protein hydrolysis by trypsin [73, 76]. Hydrolysis causes exposing the buried hydrophobic parts of proteins to the outer surface of the molecule [58, 76]. However, it is not enough to promote aggregation [73]. Soluble and discrete aggregates are formed during the hydrolysis which may not be removed by a centrifugal operation [73]. Conversely, insoluble aggregates may be segregated by centrifugation. In the present study, a very important experimental phenomenon occurred that the hydrolysates exhibited an emulsion-like appearance. It showed that sufficient hydrolysis of LP not only increased its surface hydrophobicity (LPH) but also decreased the MW and disulfide bonds of proteins, eventually transforming the insoluble native aggregates to soluble ones during the hydrolysis process [73].

According to Fig. 1, MTGase-mediated cross-linking LPH that led to the production of LPHC reduced H_0 value compared to LP and LPH. This significant decrease could be attributed to the re-burying effect of cross-linking on the exposed hydrophobic residues [43]. Indeed, the hydrolysis led to enforced exposure of hydrophobic residues, and cross-linking of LPH led to the approaching the exposed hydrophobic patches which increased the hydrophobic interactions. In other words, cross-linking reburied hydrophobic patches within the interior structure of new larger aggregates formed [43, 44, 58, 77]. Also, based on the amino acid composition shown in Table 1, a higher amount of negatively charged amino acids were found for LPHC which indicated

that the hydrophilicity of LPH was remarkably increased after cross-linking. A similar manner was observed for limited hydrolysis and conjunction of zein with chitosan oligosaccharide by MTGase-mediated reaction [43]. Indeed, covalent bond formation between two molecules reduced the accessibility of exposed hydrophobic groups which rendered reduced the H_0 value [43].

Ultrasound treatment of LPH (LPHUS) indicated a different manner compared to cross-linking (LPHC) (Fig. 1). Although sonication caused a slight reduction of H_0 value compared to LPH, the produced hydrolysates still had higher surface hydrophobicity than LP and LPHC (Fig. 1). Sonication disrupted the soluble aggregates formed during the hydrolysis process; thus, the solubility and hydrophilicity of peptides were increased [29, 53, 64]. Indeed, sonication could solely unravel the produced peptides' structure with reduction of α-helix and β-turn and increase of β-sheet in the secondary structure, disrupt the aggregates, and maintain the most of the exposed hydrophobic patches which conversely occurred compared to cross-linking process [15, 29, 53, 57]. According to the literature, pretreatment of mung bean protein with ultrasound and then its enzymatic hydrolysis led to an increase in the concentration of peptides with 0.5–1 kDa and 1–3 kDa which showed higher surface hydrophobicity and antioxidant activity [53]. Although ultrasound treatment has shown an increasing effect on the surface hydrophobicity of proteins and peptides, the hydrophobic region of the proteins or peptides might be reburied by excessive ultrasound treatment which leads to the reaggregation of protein or peptide molecules by disulfide bonds [15, 78].

MTGase-mediated cross-linking of ultrasound-treated LPH (LPHUSC) indicated a different manner compared to LPHC. Ultrasound indicated disrupting effect on the LPH, maintained the exposed hydrophobic segments, and a slight reduction of H_0 was obtained for LPHUS. Cross-linking of LPHUS exhibited a more impressive influence on the reduction of surface hydrophobicity due to the reason mentioned for LPHC [15, 58, 78]. Although sequential ultrasound treatment and then cross-linking (LPHUSC) led to a reduction of H_0 value compared to LPH and LPHUS, LPHUSC still had higher surface hydrophobicity than LPHC and no significant difference with LP (Fig. 1). Some of the disrupted aggregates via ultrasound were cross-linked through the MTGase catalyzing action and become larger and higher hydrophobic interactions led to reburying of hydrophobic patches; thus, H_0 was decreased for LPHUSC compared to LPHUS [43].

MW profile

The electrophoretic profiles of LP, LPH, LPHC, LPHUS, and LPHUSC were represented in Fig. 2. LP's electrophoretic profile indicated four intense bands at 100, 150, 170–180, and 200–230 kDa. The bands with MW higher
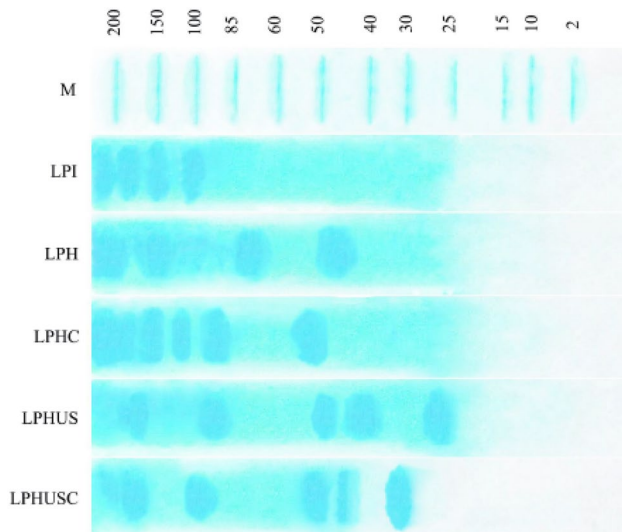
Fig. 2 SDS-PAGE patterns of LP (control), LPH, LPHC, LPHUS, and LPHUSC. LP was native lentil protein; LPH was Alcalase-Flavourzyme hydrolysates; LPHC was MTGase cross-linked LPH; LPHUS was treated LPH with ultrasound; LPHUSC was LPH treated with ultrasound and MTGase

than 85 kDa have been attributed to legumins and vicilins [33, 39]. The salt-soluble globulin fraction mainly consists of legumin ascribed to 11S, and S—Svedberg Unit with an MW of higher than 200 kDa, and vicilin 7S with an MW of 175–180 kDa [9, 33, 34, 58]. The sequential hydrolysis of LP disappeared the bands at higher than 200 kDa and 175–180 which were shifted to 200 and 150 kDa (become more intense) [10]. The band at 100 kDa was also diminished which coincided with the appearance of new intense bands at 60–85 kDa and 45–50 kDa for LPH. Legumin is a hexameric protein comprised of ~60 kDa subunits of α (~40 kDa). Also, subunits of 7S globulins such as vicilin and convicilin have shown bands at 48 kDa and 63 kDa as reported previously [10, 32, 39].

MTGase-mediated cross-linking led to the appearance of main LP bands and the bands at 60–85 kDa and 45–50 were shifted to 85–90 indicating vicilins and legumins and 50–52 kDa representing vicilin fractions, for the produced LPHC, respectively (Fig. 2) [10, 39]. Indeed, MTGase enlarged the hydrolyzed polypeptides via cross-linking. The same results were reported for soy protein hydrolysate (SPH) that was cross-linked by MTGase [44]. It was reported that MTGase catalyzed the formation of iso-peptide bonds within or among SPH peptide fragments, resulting in peptide aggregates with an increased molecular mass [44]. Also, MTGase-mediated cross-linking has shown the promotion of synthesizing a larger protein subunit (66 kDa) through new hydrogen and disulfide bonds [44, 79]

Conversely, ultrasound treatment of LPH led to the disruption of aggregated peptides (LPHUS) produced through

hydrolysis (Fig. 2) [53]. Accordingly, the bands at 200 and 150 kDa were diminished and shifted to 160, 85–90 kDa and 50 kDa, 40–42 kDa, and 25–27 kDa, respectively. The intense band at 50 kDa probably represented the subunit of vicilin (48 kDa) and the band at 40 kDa could be attributed to legumin subunit 11S (acidic subunit) [9, 39]. The band around 25–27 kDa was assigned to albumin-rich fraction peptides, contaminants with vicilin subunit 7S, and a legumin-rich fraction (basic subunit) or β chains [10, 34, 39].

Cross-linking of LPHUS (LPHUSC) led to occurrence of some shifts at bands (Fig. 2). Indeed, enlarging of peptides diminished the band at 25–27 kDa and a new intense band was formed at 29–30 kDa [44]. Also, the band at 40 kDa became thinner with a bit shift to 45 kDa. The band at 85–90 also exhibited a slight shift to 93–95 kDa.

According to the electrophoretic results of SDS-PAGE (Fig. 2), the lowest MW profile within the hydrolysate samples was obtained for LPHUS attributed to the disruption effects of the sonication process and then LPHUSC, LPH, and LPHC indicated the lower MW peptides, respectively. It was worth noting that some changes occurred at a lower MW range that was not visible on the SDS-PAGE gel [9, 10]. It could be likely due to the effects of heating on protein or peptides structures. Heating (for denaturation/unfolding of proteins/peptides and termination of enzyme) was performed during the hydrolysis and also during the preparation of samples for running the SDS-PAGE process [9, 10]. Also, it has been reported that most SDS-PAGE gels are designed to reveal MW above 10 kDa; thus, visualizing variations at MW range below 10 kDa might be achieved using a more suitable spectroscopic technique such as size exclusion chromatography (SEC) or gel permeation chromatography (GPC) [9, 15].

MW distribution

The variations in MW patterns that could not be visualized on SDS-PAGE below 10 kDa were observed by GPC, indicating the potential of GPC as a robust technique for monitoring changes in MW patterns not visible in SDS-PAGE [9, 10, 15]. The MW distribution of LP, LPH, LPHC, LPHUS, and LPHUSC was illustrated in Fig. 3. A sharp intense peak was detected for LP assigned to polypeptides with 4943 Da which could be attributed to vicilin, lectin, protease, and amylase inhibitors subunits as reported by Avramenko et al. [58]. Sequential hydrolysis of LP led to the production of peptides (LPH) with a major sharp peak assigned to MW of 1678 Da. Alcalase cleaved the LP peptide bonds broadly and medium-sized peptides were produced [10, 29, 35, 80]. After then, Alcalase-hydrolyzed LP was further cleaved by the Flavourzyme. Individual application of Flavourzyme has been demonstrated lower DH than Alcalase [27, 29]. However, when Flavourzyme was applied in the second stage
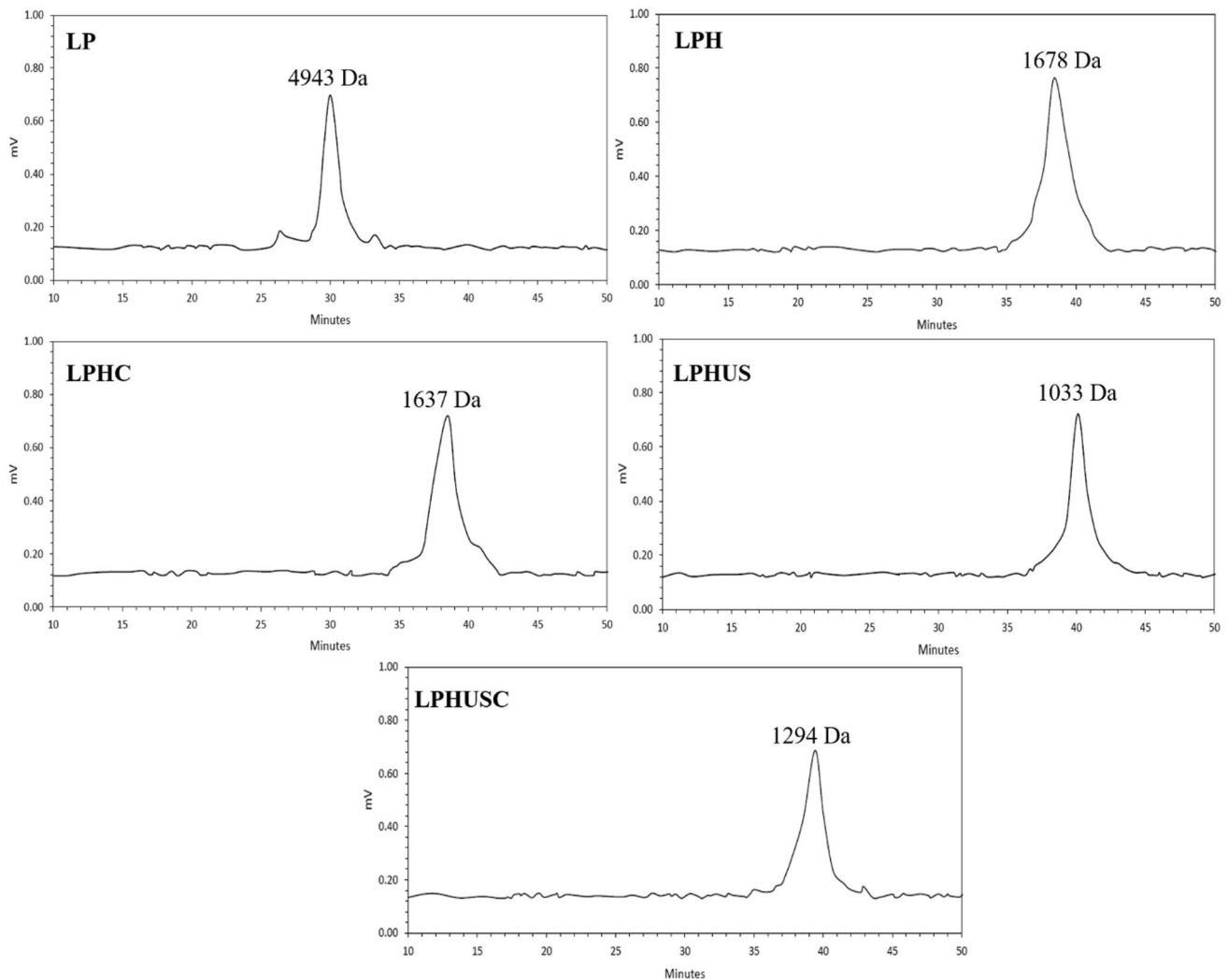
Fig. 3 MW distribution by GPC for LP (control), LPH, LPHS, LPHUS, and LPHUSC. LP was native lentil protein; LPH was Alcalase-Flavourzyme hydrolysates; LPHC was MTGase cross-linked LPH; LPHUS was treated LPH with ultrasound; LPHUSC was LPH treated with ultrasound and MTGase

of hydrolysis, the produced medium-sized peptides in the first hydrolysis stage were also degraded into small-sized peptides [9, 29]. Based on the reports, a MW less than 3 kDa peptides are mainly derived from convicilin, vicilin, and legumin containing bioactive amino acid sequences, which make them potential contributors to ACE-inhibitory and antioxidant activities [31].

Cross-linking (LPHC) did not show a significant effect on MW of LPH at lower MW ranges and the detected sharp peak was assigned to 1637 Da (Fig. 3). Although based on the SDS-PAGE pattern, MTGase-mediated cross-linking led to enlarging of hydrolyzed LP (LPH), at the lower MW range, the peptides were not efficiently cross-linked. It could be likely that large MW peptides have many specific sites for the MTGase enzyme while small MW peptides do not have sufficient sites (lysine and glutamine residues) for

enzyme cross-linking action [81]. It was worth declaring that LPH had aggregated peptides that masked the glutamine and lysine residues, especially at small MW peptides. These results followed the reports by Carvalho et al. [81] that peptides without glutamine or lysine resides may have limited cross-linking. Also, the presence of free glutamine may have prevented cross-linking [81]. Conversely, sonication led to disruption of LPH; thus, the size of peptides was markedly decreased with the detection of a sharp intense peak for LPHUS assigned to 1033 Da (Fig. 3). On another side, MTGase-mediated cross-linking of ultrasound-treated LPH (LPHUSC) altered MW distribution compared to LPHUS. Possibly, disruption of peptides by ultrasound led to increasing glutamine and lysine residues becoming accessible to the MTGase; thus, the efficiency of cross-linking was increased, and higher MW peptides were produced for

LPHUSC (Fig. 3). Accordingly, the GPC chromatogram of LPHUSC indicated a sharp peak at 1294 Da which showed that combined processes of disruption and cross-linking could change the MW distribution of peptides [82]. Ultrasound has been reported to promote cross-linking action [82]. According to the previous studies, SEC results have shown that the concentration of peptides (0.5 kDa-1 kDa and 1-3 kDa) in the hydrolysate was significantly increased after thermosonication [57].

DPPH radical scavenging activity

DPPH has been introduced as a stable free radical, which can accept protons from an antioxidant to form a stable diamagnetic molecule [10]. It is worth noting that DPPH radicals have a higher hydrophobic intention and are oil-soluble [10, 83]. According to Fig. 4a, LP indicated 12.77% DPPH RSA which could be attributed to its inherent hydrophobic peptides on the protein surface as shown by H_0 [10]. Also, the amino acid residues (Asp, Glu, Pro, Arg, His, Met, Leu, Ala, Try, and Val) might contribute to the DPPH RSA of LP. The sequential hydrolysis of LP led to a significant increase in RSA and reached 68.75% for LPH (Fig. 4a). This increase was attributed to unfolded and broken polypeptide molecules of LP. Based on the previous reports, the medium and small-sized peptides possess higher RSA against radicals [80, 83]. Alcalase generated hydrolysates have shown stronger antioxidant activity [10, 80]. When the Flavourzyme was added sequentially, the hydrolysates cleaved to smaller MW peptides and more stronger antioxidant activity was rendered [9, 10]. It has been reported that small-sized peptides have a higher chance to be adsorbed to oxidative agents [9, 10, 83]. Besides, the produced peptides had unraveled structure; thus, the buried hydrophobic segments were exposed to the surface of peptides leading to higher interaction with DPPH radicals (Figs. 1, 4a) [5, 53, 73, 76, 84, 85]. Various studies have reported that hydrolysis of proteins liberates bioactive peptides with potent antioxidant activity [9, 10, 19, 84]. Especially, Alcalase-Flavourzyme sequential hydrolysis has shown stronger RSA [9, 10]. Regarding the LPHC, a significant reduction in RSA was observed and reached 62.71% (Fig. 4a). MTGase-mediated cross-linking process led to reduction of H_0 which directly had a relation to DPPH RSA (Figs. 1, 4a). Cross-linking reaggregated the LPH and masked the hydrophobic patches with higher reactivity with DPPH radicals; thus, RSA was decreased [86]. A slight decrease was observed for LPHUS and LPHUSC which indicated 67.49 and 67.60% RSA, respectively (Fig. 4a). This decrease could also be associated with a reduction of H_0 values compared to LPH (Fig. 1). Despite this, LPHUS and LPHUSC exhibited higher RSA than LP and LPHC (Fig. 4a). Ultrasound treatment has been reported to have disrupting and unfolding effects on the aggregated peptides [53, 57]. Although disruption has led to a reduction of surface hydrophobicity of LPHUS, unraveling of spatial conformation of peptide structure could maintain the higher surface hydrophobicity value achieved for LPH (Fig. 4a). Therefore, the RSA of LPHUS and LPHUSC did not remarkably decrease compared to LPHC (Fig. 4a). All obtained hydrolysates indicated stronger DPPH RSA than that obtained from ascorbic acid (54.50%) which exhibited their potential as natural preservatives to be used in food formulations [9, 10].
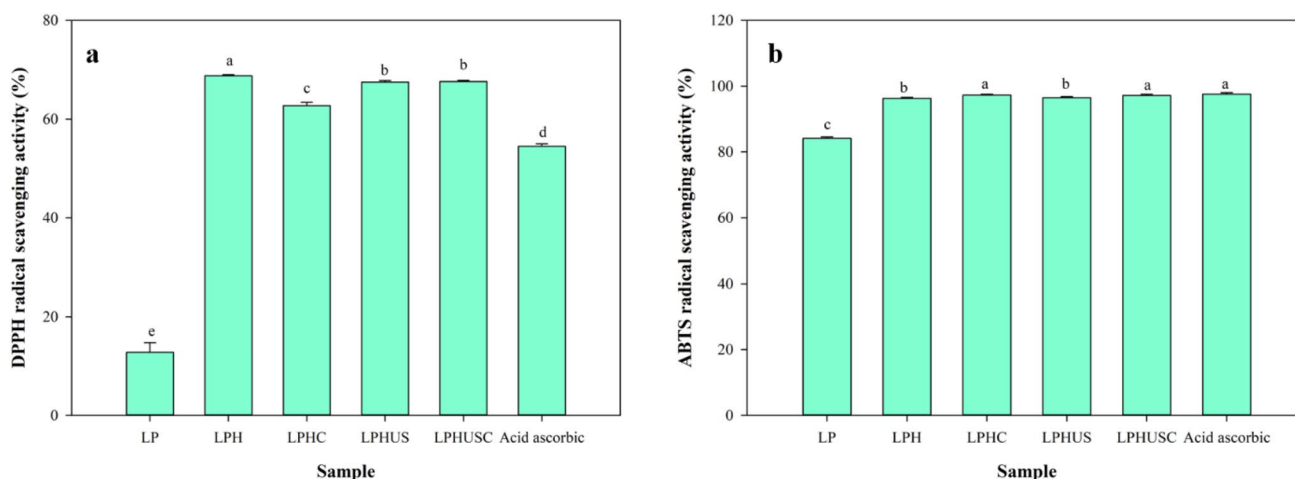

Fig. 4 Antioxidant activity of LP, LPH, LPHC, LPHUS, and LPHUSC by DPPH (**a**) and ABTS (**b**) radical scavenging activities (RSA). LP was native lentil protein; LPH was Alcalase-Flavourzyme hydrolysates; LPHC was MTGase cross-linked LPH; LPHUS was treated LPH with ultrasound; LPHUSC was LPH treated with ultrasound and MTGase

ABTS radical scavenging activity

ABTS radicals have been recognized as water-soluble radicals which can be efficiently interacted with hydrophilic antioxidants [83]. According to Fig. 4b, LP indicated 84.14% RSA while sequential hydrolysis led to a significant increase in ABTS RSA reaching 96.25% RSA for LPH. The higher ABTS RSA of LP could be attributed to higher hydrophilic amino acid residues [83]. Sequential hydrolysis led to the production of small-sized peptides which have been reported to be efficiently adsorbed to radicals [10, 83]. Also, reduction of molecular size can increase the solubility which leads to higher interaction with ABTS hydrophilic radicals [59]. The same results were obtained for date seed hydrolysates prepared using Alcalase and Flavourzyme [59]. MTGase-mediated cross-linking (LPHC) led to a slight increase (97.28% RSA) compared to LPH (Fig. 4b). This could be attributed to the reduction of the H_0 value of LPHC and relatively higher hydrophilic interactions occurred with ABTS radicals which increased RSA. Ultrasound treatment could maintain hydrophobic/hydrophilic balance and higher DPPH and ABTS RSA values were achieved for LPHUS. Ascorbic acid also indicated 97.60% RSA which showed that the peptides obtained from LP can be potentially substituted with it in food formulations.

Anti-hypertension activity

ACE-inhibitory results were represented in Fig. 5a. LP indicted 57.35% inhibition which was in agreement with that reported in the recent studies [9, 10]. Sequential hydrolysis led to a significant increase in antihypertension activity and ACE-inhibitory activity reached 70.73% for LPH (Fig. 5a) [9, 10]. Degradation of LP into medium- and small-sized peptides led to the liberation of active antihypertensive sequences of amino acids [31, 39]. Similar results were recorded in the previous studies [9, 10, 39]. Garcia-Mora et al. [32] reported that ACE-inhibition ranged between 40 to 57% for LPH which was produced by high pressure-assisted proteolysis by Alcalase. In most cases, the peptides with MW less than 3000 Da have shown higher anti-hypertension activity [9, 10, 32, 84]. Also, the enriched legumin (119 ± 0.5 μmol/L), albumin (127 ± 2 μmol/L), and vicilin (135 ± 2 μmol/L) fractions in LPH have been reported to render the highest ACE-inhibitory activity [39].

MTGase-mediated cross-linking also increased ACE inhibition and reached 86% for LPHC (Fig. 5a). It could be related to the association of some peptides that highly interacted with ACE. Although LPHC had the peptides with MW of 1637 Da detected by GPC chromatogram, the higher MW peptides around 50 kDa respected to vicilin fractions were also detected by the SDS-PAGE electrophoretic pattern (Figs. 2, 3). The collection of these peptides gave rise to higher inhibition of ACE. Different range of MW has been reported for ACE-inhibition and also other biological activities. The biological activities are highly associated with specific peptide sequences in hydrolysates. Digestion of bean (*Phaseolus vulgaris* L.) seeds released peptide fractions with MW of 3.5–7 kDa which indicated the highest ACE-inhibitory activity [87].

Ultrasound treatment of LPH (LPHUS) led to an increase in ACE-inhibitory activity (78.32%) compared to individual LPH (Fig. 5a). Each treatment produced a different sequence of peptides with different amino acids; thus, different biological activities were presented. According to the SDS-PAGE profile and GPC chromatogram results (Figs. 2, 3), a combination of peptides indicated a specific ACE inhibition.

The determined IC_{50} values were 0.91, 0.48, 0.27, 0.33, and 0.23 mg/mL for LP, LPH, LPHC, LPHUS, and LPHUSC, respectively. Different IC_{50} values have been found in the literature based on the enzyme employed in hydrolysis. The lowest IC_{50} value indicated a higher inhibition of ACE. The reported IC_{50} values ranged between 0.15 to 0.44 mg/mL for LPH without cross-linking or ultrasound-treated LPH [10, 31, 34, 88].
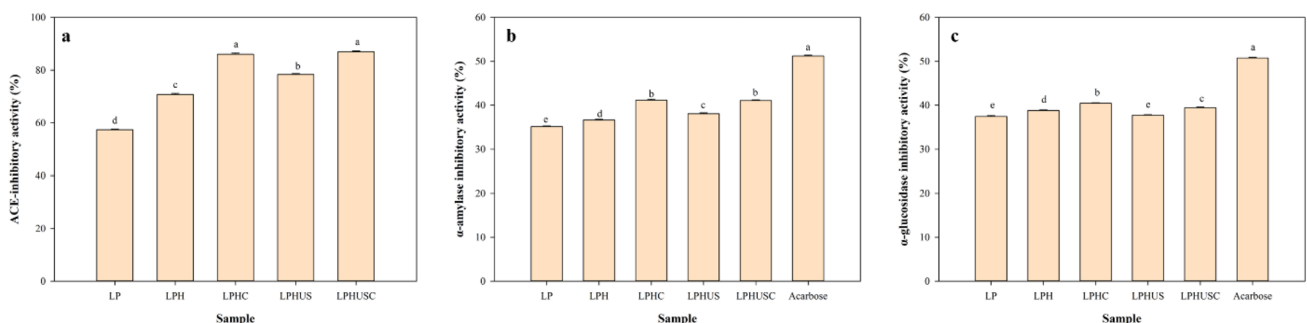

Fig. 5 ACE (**a**), α-amylase (**b**), and α-glucosidase (**c**) inhibitory activities of LP, LPH, LPHC, LPHUS, and LPHUSC. LP was native lentil protein; LPH was Alcalase-Flavourzyme hydrolysates; LPHC was MTGase cross-linked LPH; LPHUS was treated LPH with ultrasound; LPHUSC was LPH treated with ultrasound and MTGase

Antidiabetic activity

One of the strategies to control type 2 diabetes is the use of synthetic medicines like acarbose and voglibose [28]. They suppress the absorption of glucose by indicating inhibition effects on α-amylase and α-glucosidase [28]. The α-amylase is an enzyme that hydrolyses alpha-bonds (internal alpha-1,4-glucan links) of polysaccharides such as glycogen and starch to yield glucose and maltose [28, 89]. The α-glucosidase cleaves the disaccharides and releases glucose molecules [15, 36]. The reduction of glucose levels in the blood by the inhibition of α-amylase is known as in vitro indicator of controlling diabetes [36, 68]. Although these drugs can efficiently show inhibiting effects on the respective enzymes, they suffer from high cost and also gastrointestinal side effects like diarrhea (14% of patients) and flatulence (78% of patients) [28].

The α-amylase and α-glucosidase inhibitory activities of LP, LPH, LPHC, LPHUS, and LPHUSC were represented in Fig. 5bc. Regarding the α-amylase inhibitory activity (Fig. 5b), LP indicated 35.13% inhibition. The sequential hydrolysis led to a slight increase and reached 36.63% for LPH. The most efficient process was MTGase-mediated cross-linking of LPH which led to the α-amylase inhibitory activity of 41.16% for LPHC. Also, ultrasound treatment increased the α-amylase inhibitory activity compared to LP and LPH and reached 38.06% for LPHUS. The LPHUSC indicated 41.06% inhibition without significant difference with LPHC. Acarbose is the synthetic drug for diabetes Mellitus control indicated the highest α-amylase inhibitory acidity (51%) which could be related to its purity [3]. The produced hydrolysates had a variety of antidiabetic and nonantidiabetic sequences of peptides; thus, they exhibited lower α-amylase inhibitory activity than that obtained for acarbose. The 50% α-amylase inhibitory concentrations (IC_{50}) were 4.22, 2.51, 1.35, 1.95, 1.16, and 0.43 mg/mL for LP, LPH, LPHC, LPHUS, LPHUSC, and acarbose, respectively. The α-amylase inhibition of LP and produced hydrolysates were higher than lupin protein and its hydrolysates produced by Alcalase and Flavourzyme [15]. This difference could be attributed to a different sequence of proteins/peptides with different amino acid residues [15]. The bioactive peptides can bind or interact with the enzyme's active site and inhibit the interaction between the enzyme and substrate [3, 15]. Furthermore, bioactive peptides can bind to the allosteric site of the enzyme, for instance, calcium and chloride ion sites, and create an unstable conformation, restricting the displacement of the enzyme on the substrate [3]. Indeed, calcium ions have crucial roles in the structure, function, and stability of α-amylase [3]. Removal of calcium ions can inactivate the enzyme. Besides, amino acids including aspartic and glutamic acids, glycine, leucine, serine, proline, phenylalanine, tryptophan, and tyrosine have been reported likely to bind active domains and indicate a potential to inhibit the enzyme [3]. According to the literature, using Flavourzyme led to the production of peptides with higher α-amylase inhibition [15]. Rahimi et al. [36] reported that potato protein hydrolysates (obtained by Alcalase) with high MW peptides indicted higher α-amylase inhibition. Also, the ability of peptides to interact through hydrophobic interactions with the active site of enzymes has been demonstrated to be the mechanism behind the inhibitory action of peptides [15, 36]. The determined values of α-amylase inhibitory activities indicated that LP, LPH, and processed LPH samples can be potentially used as antidiabetic agents especially when the specific fractions become separated (Fig. 5b). LPHC and LPHUSC were the most efficient peptides for the inhibition of α-amylase.

Regarding the α-glucosidase inhibitory activity (Fig. 5c), LP indicated 37.45% inhibition while hydrolysis led to a slight increase and reached 38.80% for LPH. MTGase-mediated cross-linking increased α-glucosidase inhibitory activity a bit more and reached 40.43% for LPHC. LPHUSC indicated 39.41% inhibition which was higher than LP, LPH, and LPHUS and lower than LPHC. Acarbose is a synthetic drug for diabetes control indicating 50.75% inhibition which was related to its high purity. Also, the IC_{50} values were 2.58, 1.74, 1.20, 1.75, 1.23, and 0.51 mg/mL for LP, LPH, LPHC, LPHUS, LPHUSC, and acarbose, respectively. Molecular docking analyses revealed that the α-glucosidase inhibition by the peptides could be mainly attributed to the formation of five strong hydrogen bonds between Glu-Ala-Lys and His-674, Asp-518, Arg-600, Asp-616, and Asp-282 in α-glucosidase, and four hydrogen bonds between Gly-Ser-Arg and residues Asp-282, Asp-518, and Asp-616 [90]. However, in the present samples, different peptides with different amino acid sequences have shown different results. A higher DH value has also been reported rendering higher antidiabetic and α-glucosidase inhibitory activity [91]. The higher inhibition for LPHC and LPHUSC could be associated with the production of a range of small- and medium-sized peptides with MW less than 100 kDa [85]. The amino acid residues have also been reported to efficiently influence the α-glucosidase inhibitory activity [15, 36]. The determined α-glucosidase inhibitory activities exhibited that LP and its hydrolysates can be efficiently used as antidiabetic agents especially when the peptides become fractionated.

Functional properties

The determined values of solubility, EAI, ESI, FC, and FS were provided in Table 2. Regarding the solubility, LP indicated no solubility at pH values of 4.0 and 7.0 attributed to lack of electrostatic repulsion at pH 4.0 (isoelectric point) and inherent hydrophobic surface of intact protein at pH 7.0. pH shifting to 9.0 significantly increased the solubility

Table 2 Functional properties of LP, LPH, LPHC, LPHUS, and LPHUSC

Sample	Solubility (%)			EAI (m^2/g)	ESI (min)	FC (%)	FS (%) after 30 min
	pH 4	pH 7	pH 9				
LP	00.00 ± 00.00^{Bd}	00.00 ± 0.00^{Bd}	56.00 ± 0.00^{Ad}	49.10 ± 0.50^{b}	21.80 ± 2.30^{d}	80.10 ± 2.10^{b}	57.89 ± 0.20^{a}
LPH	92.00 ± 01.30^{Bb}	96.00 ± 0.00^{Ac}	96.00 ± 0.00^{Ab}	29.47 ± 1.20^{d}	10.30 ± 0.50^{e}	90.00 ± 1.50^{a}	48.71 ± 3.40^{b}
LPHC	96.00 ± 01.20^{Ca}	98.00 ± 0.00^{Bb}	100.0 ± 0.00^{Aa}	38.50 ± 1.50^{c}	67.41 ± 3.40^{b}	46.15 ± 2.30^{e}	12.82 ± 1.30^{d}
LPHUS	86.00 ± 02.10^{Cc}	98.00 ± 0.00^{Ab}	94.00 ± 0.00^{Bc}	25.79 ± 2.10^{e}	100.0 ± 0.00^{a}	53.84 ± 1.40^{d}	23.07 ± 2.10^{c}
LPHUSC	92.00 ± 02.10^{Bb}	100.0 ± 0.00^{Aa}	100.0 ± 0.00^{Aa}	55.27 ± 1.30^{a}	51.72 ± 3.20^{c}	65.00 ± 1.90^{c}	10.00 ± 0.20^{e}

The different small and large superscripts indicate significant differences among the columns and rows ($p < 0.05$)

and reached 56% for LP which could be attributed to the increase of negative charge on the protein surface; thus, an increase in electrostatic repulsion led to higher solubility [9, 10, 43]. Hydrolysis of LP and subsequent processing methods resulted in higher solubility at the 3 mentioned pH values (Table 2). LPH indicated solubility values of 92, 96, and 96%, LPHC indicated 96, 98, and 100%, LPHUS exhibited 86, 98, and 94%, and LPHUSC showed 92, 100, and 100% at pH values of 4.0, 7.0, and 9.0, respectively [10, 38, 92]. Most alterations were observed at pH 4.0 attributed to changes in particle charges and surface hydrophilicity and hydrophobicity of produced peptides [38]. MTGase-mediated cross-linking indicated a rising effect on the solubility while sonication (LPHUS and LPHUSC) slightly reduced the solubility, especially at a pH of 4.0 (Table 2). Changes in MW altered the hydrophilicity and hydrophobicity of peptides and different solubility values were observed [10].

Regarding the emulsifying attributes, LP indicated EAI of 49.10 m^2/g which declined to 29.47 m^2/g for LPH (Table 2). LP due to possessing highly hydrophobic patches in the protein structure has been introduced as a good emulsifier [75, 93]. It is noteworthy that emulsifying activity not only depends on the surface hydrophobic activity of proteins but also on their hydrophilicity [10]. When a protein tends to be adsorbed to the interface of oil–water by mechanical enforcement, it should have first high solubility in water. Then, the adsorbed protein with its surface activity disperses the oil within the continuous phase [56]. Also, exposed non-degraded proteins (by thermal or non-thermal denaturing) have shown higher EAI compared to intact non-degraded proteins [10, 56]. Although sequential hydrolysis by Alcalase and Flavourzyme led to an increase in H_0 value and solubility, due to the reduction of molecular mass, there were not sufficient proteins at the interface to drag the oil droplets and enforce them to be distributed within the continuous phase [7, 56]. Indeed, hydrolysis increased the aggregation of soluble peptides which were not efficiently adsorbed to the interface [10, 56, 73]. MTGase-mediated cross-linking led to a significant increase in EAI and reached 38.50 m^2/g (Table 2). Cross-linking likely formed peptides with well-balanced hydrophilic/hydrophobic properties which

exhibited higher EAI than LPH [58, 77]. On another side, enlarging the peptides supported the improvement of surface interfacial tension attributes which led to the efficient fabrication of emulsion [44, 94]. Similar results were found for soy protein hydrolysates obtained by Alcalase and cross-linked with MTGase [44]. Ultrasound treatment of LPH led to a significant reduction of EAI which reached 25.79 m^2/g for LPHUS (Table 2). It could be attributed to the disruption effects of sonication on the aggregated peptides and the reduction of MW. Therefore, it could be declared that MW exhibited a fundamental role in EAI. The highest EAI, 55.27 m^2/g was achieved for LPHUSC (Table 2). The combined sonication and cross-linking likely formed peptides with higher interfacial tension activity. Ultrasound treatment first disrupted the aggregates then cross-linking rearranged them with higher surface activity associated with enlarged MW of peptides [44]. The ESI values were 21.80, 10.30, 67.41, 100, and 51.72 min for LP, LPH, LPHC, LPHUS, and LPHUSC, respectively. Hydrolysis led to a reduction of ESI while cross-linking and sonication significantly improved the ESI corresponding to the formation of new peptides with strong electrostatic repulsion and lower particle size (Table 2) [10, 44, 49, 54, 56].

Regarding the foaming properties (Table 2), LP indicated 80.10% FC while reaching 90% for LPH. Lower molecular size peptides with higher solubility have shown higher FC than large peptides [10, 92]. Indeed, the adsorption of small peptides into the interface of air–water was facilitated [10, 92]. MTGase-mediated cross-linking led to a reduction of LPH's FC reaching 46.15% for LPHC [44]. It could be likely attributed to enlarging effects that increased the MW of peptides and FC was decreased. Ultrasound treatment of LPH also decreased FC for LPHUS (53.84%) compared to LP and LPH. Possibly more reduction of MW led to lower foam production [10]. Combined sonication and cross-linking (LPHUSC) resulted in higher FC (65%) than individual cross-linking (LPHC) and sonication (LPHUS) (Table 2). Regarding the FS, the obtained values were 57.89, 48.71, 12.82, 23.07, and 10% for LP, LPH, LPHC, LPHUS, and LPHUSC, respectively. As shown in Table 2, FS was significantly decreased by hydrolysis and more reduced by

further processing. It could be attributed to the formation of new peptides with smaller MWs which indicated a lower ability in maintaining the foam [9, 44, 58]. In more details, cross-linking and sonication led to a reduction of FC and FS values. Regarding the cross-linking, formation of new peptide aggregates reduced the surface hydrophobicity of peptides; thus, weaker interactions occurred with oxygen at the air–water interface [44]. Ultrasound treatment also slightly reduced the surface hydrophobicity and lower FC was obtained. However, as mentioned, combined cross-linking and sonication treatment (LPHUSC) led to a significant increase in FC while the lowest FS was obtained for LPHUSC (Table 2). Also, higher DH (36%) impaired foaming properties [10, 58]. It has been reported that excessive hydrolysis makes the hydrolysates more hydrophilic disturbing the hydrophilic/hydrophobic balance which results in decreasing foam formation and stability [10, 44, 65].

Conclusion

The potent antioxidant, anti-hypertension, and antidiabetic peptides were produced through sequential hydrolysis of LP via Alcalase-Flavourzyme, cross-linking by MTGase, and sonication. Amino acid profiles were maintained after processes and slight changes were observed for residual values. The highest H_0 value was obtained for LPH. Cross-linking of LPH indicated a decreasing effect on H_0 while ultrasound exhibited maintaining influence. Hydrolysis of LP (LPH) and sonication of LPH (LPHUS) decreased MW while cross-linking of LPH indicated enlarging effect. A higher hydrophobicity value led to higher DPPH RSA for LPH, LPHUS, and LPHUSC. The reduction of MW led to higher ABTS RSA for all hydrolysate samples. The highest ACE, α-amylase, and, α-glucosidase inhibitory activities were obtained for LPHC and LPHUSC. Hydrolysis led to a reduction of EAI while combined cross-linking and sonication led to improvement of it.

This study indicated that processed LPH can be substituted by chemical antioxidants, reducing blood pressure drugs, and antidiabetic drugs. Albeit, further research studies are needed to investigate the effects of modified LPH on human health, evaluation of digestibility in gastrointestinal conditions, and investigate the possible applications of the modified LPH in the food sector.

Data availability All data generated or analyzed during this study are included in this published article.

Declarations

Conflict of interest The authors declare no conflict of interest.

References

1. R. Han, A.J. Hernández Álvarez, J. Maycock, B.S. Murray, C. Boesch, Curr. Res. Food Sci. **4**, 141 (2021)
2. B. P. Singh, R. E. Aluko, S. Hati, D. Solanki, Crit. Rev. Food Sci. Nutr. (2021)
3. A. Karimi, M.H. Azizi, H. Ahmadi Gavlighi, Food Sci. Nutr. **8**, 2395 (2020)
4. C. Ozuna, I. Paniagua-Martínez, E. Castaño-Tostado, L. Ozimek, S.L. Amaya-Llano, Food Res. Int. **77**, 685 (2015)
5. M. Hayta, B. Benli, E.M. İşçimen, A. Kaya, J. Food Meas. Charact. **14**, 2578 (2020)
6. Z. Emam-Djomeh, A. Rezvankhah, in *Release Bioavailab. Nanoencapsulated Food Ingredients* (Elsevier, 2020), pp. 79–120.
7. A. Rezvankhah, Z. Emam-Djomeh, M. Safari, M. Salami, G. Askari, J. Food Process. Preserv. e16554 (2022)
8. A. Marciniak, S. Suwal, N. Naderi, Y. Pouliot, A. Doyen, Trends Food Sci. Technol. **80**, 187 (2018)
9. A. Rezvankhah, M.S. Yarmand, B. Ghanbarzadeh, H. Mirzaee, J. Food Process. Preserv. **45**, e15932 (2021)
10. A. Rezvankhah, M.S. Yarmand, B. Ghanbarzadeh, H. Mirzaee, J. Food Meas. Charact. **15**, 5021 (2021)
11. S.M.T. Gharibzahedi, B. Smith, Trends Food Sci. Technol. **107**, 466 (2021)
12. L. Sha, Y.L. Xiong, Trends Food Sci. Technol. **102**, 51 (2020)
13. S. Chandrasekaran, E. Gonzalez de Mejia, Food Chem. **374**, 131717 (2022)
14. I.U. Okagu, T.P.C. Ezeorba, E.C. Aham, R.N. Aguchem, R.N. Nechi, Food Chem. Mol. Sci. **4**, 100078 (2022)
15. G.J. Fadimu, H. Gill, A. Farahnaky, T. Truong, Food Chem. **383**, 132457 (2022)
16. E. Elam, J. Feng, Y.M. Lv, Z.J. Ni, P. Sun, K. Thakur, J.G. Zhang, Y.L. Ma, Z.J. Wei, J. Funct. Foods **86**, 104674 (2021)
17 W. Song, X. Kong, Y. Hua, Y. Chen, C. Zhang, Y. Chen, Lwt **125**, 109199 (2020)
18. A.M. Reyes Jara, C.S. Liggieri, M.A. Bruno, Food Chem. **264**, 326 (2018)
19. J.A. do Evangelho, N.L. Vanier, V.Z. Pinto, J.J.D. Berrios, A.R.G. Dias, E.R. da Zavareze, Food Chem. **214**, 460 (2017)
20 S.F. Wong, B.Q. Lee, K.H. Low, H.S. Jenatabadi, C.W.J.B. Wan Mohamed Radzi, S.M. Khor, Food Chem. **311**, 129801 (2020)
21 J. Adler-Nissen, J. Chem. Technol. Biotechnol. Biotechnol. **34B**, 215 (1984)
22. J. Adler-Nissen, J. Agric. Food Chem. **27**, 1256 (1979)
23. S. Meng, Y. Tan, S. Chang, J. Li, S. Maleki, N. Puppala, Food Chem. **302**, 125186 (2020)
24. X. Gong, X. Hui, G. Wu, J.D. Morton, M.A. Brennan, C.S. Brennan, Food Res. Int. **152**, 110715 (2022)
25. L. Liu, J. Chen, X. Li, Process Biochem. **111**, 200 (2021)
26 S. Ghelich, P. Ariaii, M. Ahmadi, Int. J. Pept. Res. Ther. **28**, 1 (2022)
27. C.K. Wei, K. Thakur, D.H. Liu, J.G. Zhang, Z.J. Wei, Food Chem. **263**, 186 (2018)
28. V.G. Tacias-Pascacio, R. Morellon-Sterling, E.H. Siar, O. Tavano, Á. Berenguer-Murcia, R. Fernandez-Lafuente, Int. J. Biol. Macromol. **165**, 2143 (2020)
29. G.J. Fadimu, H. Gill, A. Farahnaky, T. Truong, Food Bioprocess Technol. **14**, 2004 (2021)
30. W.Y. Liu, L. Fang, X.W. Feng, G.M. Li, R.Z. Gu, Eur. Food Res. Technol. **246**, 2017 (2020)
31. P. Garcia-Mora, E. Peñas, J. Frias, C. Martínez-Villaluenga, J. Agric. Food Chem. **62**, 4166 (2014)
32. P. Garcia-Mora, E. Peñas, J. Frias, R. Gomez, C. Martinez-Villaluenga, Food Chem. **171**, 224 (2015)
33. C. Barbana, A.C. Boucher, J.I. Boye, Food Res. Int. **44**, 174 (2011)

34. C. Barbana, J.I. Boye, Food Chem. **127**, 94 (2011)
35. L. Ramírez Fuentes, C. Richard, L. Chen, J. Funct. Foods **87**, 104829 (2021)
36. R. Rahimi, H. Ahmadi Gavlighi, R. Amini Sarteshnizi, M. Barzegar, C.C. Udenigwe, LWT **154**, 112765 (2022)
37. A.N.A. Aryee, J.I. Boye, Int. J. Food Prop. **19**, 2649 (2016)
38. Y. Xu, M. Galanopoulos, E. Sismour, S. Ren, Z. Mersha, P. Lynch, A. Almutaimi, J. Food Meas. Charact. **14**, 343 (2020)
39. J.I. Boye, S. Roufik, N. Pesta, C. Barbana, LWT-Food Sci. Technol. **43**, 987 (2010)
40. M. Joshi, B. Adhikari, P. Aldred, J.F. Panozzo, S. Kasapis, Food Chem. **129**, 1513 (2011)
41. M.G. Nosworthy, G. Medina, A.J. Franczyk, J. Neufeld, P. Appah, A. Utioh, P. Frohlich, J.D. House, Food Chem. **240**, 588 (2018)
42. A.L.C. Gaspar, S.P. De Góes-Favoni, Food Chem. **171**, 315 (2015)
43. W. He, L. Tian, F. Fang, D. Chen, E. Federici, S. Pan, O.G. Jones, Food Chem. **348**, 129035 (2021)
44. Q. Zhang, Z. Cheng, Y. Wang, S. Zheng, Y. Wang, L. Fu, LWT **151**, 112096 (2021)
45. N. Song, C. Tan, M. Huang, P. Liu, K. Eric, X. Zhang, S. Xia, C. Jia, Food Chem. **136**, 144 (2013)
46. R.C. Viscarra-Torrico, A. Pajak, A.S. Garzón, B.L. Zhang, S. Pandurangan, M. Diapari, Q. Song, R.L. Conner, J.D. House, P.N. Miklas, A. Hou, F. Marsolais, Legum. Sci. **3**, e103 (2021)
47. X.L. Liu, C.L. Song, J.P. Chen, X. Liu, J. Ren, X.Q. Zheng, Foods **9**, 555 (2020)
48. X. Dong, J. Wang, V. Raghavan, Crit. Rev. Food Sci. Nutr. **337**, 127811 (2021)
49. W. Zhang, L. Huang, W. Chen, J. Wang, S. Wang, Ultrason. Sonochem. **73**, 105546 (2021)
50. L. Mirmoghtadaie, S. ShojaeeAliabadi, S.M. Hosseini, Food Chem. **199**, 619 (2016)
51. L. Abadía-García, E. Castaño-Tostado, L. Ozimek, S. Romero-Gómez, C. Ozuna, S.L. Amaya-Llano, Innov. Food Sci. Emerg. Technol. **37**, 84 (2016)
52. C. Wen, J. Zhang, H. Zhang, Y. Duan, H. Ma, Food Chem. **299**, 125165 (2019)
53. R. Tian, J. Feng, G. Huang, B. Tian, Y. Zhang, L. Jiang, X. Sui, Ultrason. Sonochem. **68**, 105202 (2020)
54. L. Chen, J. Chen, J. Ren, M. Zhao, J. Agric. Food Chem. **59**, 2600 (2011)
55. M. Dabbour, R. He, B. Mintah, M.K. Golly, H. Ma, J. Food Process. Preserv. **44**, e14398 (2020)
56. A. Rezvankhah, Z. Emam-Djomeh, G. Askari, Dry. Technol. **38**, 235 (2020)
57. J. Ashraf, L. Liu, M. Awais, T. Xiao, L. Wang, X. Zhou, L.T. Tong, S. Zhou, Ultrason. Sonochem. **66**, 105121 (2020)
58. N.A. Avramenko, N.H. Low, M.T. Nickerson, Food Res. Int. **51**, 162 (2013)
59. P. Ambigaipalan, A.S. Al-Khalifa, F. Shahidi, J. Funct. Foods **18**, 1125 (2015)
60. F. Rivero-Pino, F.J. Espejo-Carpio, E.M. Guadix, Food Biosci. **44**, 101328 (2021)
61. X. Zhou, H. Cui, Q. Zhang, K. Hayat, J. Yu, S. Hussain, M.U. Tahir, X. Zhang, C.T. Ho, Food Res. Int. **140**, 109985 (2021)
62. B. Cabanillas, M.M. Pedrosa, J. Rodríguez, Á. González, M. Muzquiz, C. Cuadrado, J.F. Crespo, C. Burbano, Mol. Nutr. Food Res. **54**, 1266 (2010)
63. X. Kou, J. Gao, Z. Zhang, H. Wang, X. Wang, LWT-Food Sci. Technol. **50**, 591 (2013)
64. C. Zhou, J. Hu, X. Yu, A.E.G.A. Yagoub, Y. Zhang, H. Ma, X. Gao, P.N.Y. Otu, LWT **77**, 488 (2017)
65. I. Fatollahy, J. Farmani, M.R. Kasaai, H. Hamishehkar, LWT **140**, 110765 (2021)
66. M. Venuste, X. Zhang, C.F. Shoemaker, E. Karangwa, S. Abbas, P.E. Kamdem, Food Funct. **4**, 811 (2013)
67. L. You, M. Zhao, C. Cui, H. Zhao, B. Yang, Innov. Food Sci. Emerg. Technol. **10**, 235 (2009)
68. Y.Y. Ngoh, C.Y. Gan, Food Chem. **190**, 331 (2016)
69. L. Jiang, J. Wang, Y. Li, Z. Wang, J. Liang, R. Wang, Y. Chen, W. Ma, B. Qi, M. Zhang, Food Res. Int. **62**, 595 (2014)
70. Y. Zhao, X. Zhao, D. Sun-Waterhouse, G. Ivan Neil Waterhouse, M. Zhao, J. Zhang, F. Wang, G. Su, Food Chem. **345**, 128803 (2021)
71. V. Joshi, S. Kumar, Int. J. Food Ferment. Technol. **5**, 107 (2015)
72. X. Liu, X. Zheng, Z. Song, X. Liu, N. Kumar Kopparapu, X. Wang, Y. Zheng, J. Funct. Foods **18**, 1147 (2015)
73. X.Q. Zheng, J.T. Wang, X.L. Liu, Y. Sun, Y.J. Zheng, X.J. Wang, Y. Liu, Food Chem. **172**, 407 (2015)
74. M. Primozic, A. Duchek, M. Nickerson, S. Ghosh, Food Hydrocoll. **77**, 126 (2018)
75. M. Joshi, B. Adhikari, P. Aldred, J.F. Panozzo, S. Kasapis, C.J. Barrow, Food Chem. **134**, 1343 (2012)
76. A.M. Shi, B. Jiao, H.Z. Liu, S. Zhu, M. Jiang Shen, X.L. Feng, H. Hu, L. Liu, S. Faisal, Q. Wang, B. Adhikari, Lwt **97**, 662 (2018)
77. C. Liu, S. Damodaran, M. Heinonen, Lwt **99**, 396 (2019)
78. H. Cao, R. Sun, J. Shi, M. Li, X. Guan, J. Liu, K. Huang, Y. Zhang, Ultrason. Sonochem. **77**, 105685 (2021)
79. J. Zhang, Q. Chen, L. Liu, Y. Zhang, N. He, Q. Wang, Food Hydrocoll. **112**, 106346 (2021)
80. Y.Y. Wang, C.Y. Wang, S.T. Wang, Y.Q. Li, H.Z. Mo, J.X. He, Food Chem. **345**, 128765 (2021)
81. N. de Carvalho, T.B. Pessato, F. Negrão, M.N. Eberlin, J.H. Behrens, R.L. de Zollner, F.M. Netto, LWT **113**, 108291 (2019)
82. W. Zhang, P. Zhao, J. Li, X. Wang, J. Hou, Z. Jiang, Ultrason. Sonochem. **83**, 105935 (2022)
83. R. Hu, G. Chen, Y. Li, Molecules **25**, 4091 (2020)
84. J. Xie, M. Du, M. Shen, T. Wu, L. Lin, Food Chem. **270**, 243 (2019)
85. R. Amini Sarteshnizi, M.A. Sahari, H. Ahmadi Gavlighi, J.M. Regenstein, M. Nikoo, C.C. Udenigwe, LWT **142**, 111019 (2021)
86. C. Sonklin, N. Laohakunjit, O. Kerdchoechuen, K. Ratanakhanokchai, J. Food Sci. Technol. **55**, 265 (2018)
87. A. Jakubczyk, M. Karaś, U. Złotek, U. Szymanowska, Food Res. Int. **100**, 489 (2017)
88. F. Roy, J.I. Boye, B.K. Simpson, Food Res. Int. **43**, 432 (2010)
89. Z. Yu, W. Yin, W. Zhao, J. Liu, F. Chen, Food Chem. **135**, 2078 (2012)
90. M. Jiang, H. Yan, R. He, Y. Ma, Eur. Food Res. Technol. **244**, 1995 (2018)
91. R. Wang, H. Zhao, X. Pan, C. Orfila, W. Lu, Y. Ma, Food Sci. Nutr. **7**, 1848 (2019)
92. V. García Arteaga, M. Apéstegui Guardia, I. Muranyi, P. Eisner, U. Schweiggert-Weisz, Innov. Food Sci. Emerg. Technol. **65**, 102449 (2020)
93. Z. Ma, J.I. Boye, B.K. Simpson, S.O. Prasher, D. Monpetit, L. Malcolmson, Food Res. Int. **44**(8), 2534–2544 (2011)
94. X.X. Yu, C. Liu, M.H. Lu, Y. Le Liu, J.Y. Yin, Y.H. Zhang, Food Funct. **10**, 1653 (2019)